





## RESEARCH ARTICLE

# Chemical Composition, Anti-Inflammatory Effect, and Molecular Docking of Essential Oils Extracted From *Illigera celebica* Hance. (Hernandiaceae)

Trang Huyen Xuan Hoang<sup>1</sup> | The-Huan Tran<sup>1</sup> | Tuan Quoc Doan<sup>1,2</sup>  | Anh Tuan Le<sup>3</sup>  | Hoai Thi Nguyen<sup>1</sup>  | Linh Thuy Thi Tran<sup>1</sup> 

<sup>1</sup>Faculty of Pharmacy, Hue University of Medicine and Pharmacy, Hue University, Hue City, Vietnam | <sup>2</sup>Graduate School of Environmental, Life, Natural Science and Technology, Okayama University, Okayama City, Japan | <sup>3</sup>Mien Trung Institute for Scientific Research, Vietnam Academy of Science and Technology, Hue City, Vietnam

**Correspondence:** Linh Thuy Thi Tran ([tranthithuylinh@hueuni.edu.vn](mailto:tranthithuylinh@hueuni.edu.vn))

**Received:** 26 March 2025 | **Revised:** 13 June 2025 | **Accepted:** 2 July 2025

**Funding:** Tran The Huan was funded by the Master PhD Scholarship Programme of Vingroup Innovation Foundation (VINIF), code VINIF.2024.TS.053.

**Keywords:** bioactive plant volatiles | GC–MS profiling | multi-target docking | nitric oxide inhibition | sesquiterpenes

## ABSTRACT

*Illigera celebica* Hance is an evergreen climber found in China and Southeast Asia. This study investigates the chemical composition, nitric oxide (NO) inhibitory activity, and molecular mechanisms of essential oils from *I. celebica* in Vietnam. Gas chromatography–mass spectrometry analysis identified 20 compounds, mainly aldehydes and oxygenated sesquiterpenes. Leaf oil was dominated by dodecanal (65.9%), while khusimone (31.5%) was the major compound in stem oil. In LPS-stimulated RAW 264.7 cells, the oils showed significant NO inhibition, with IC<sub>50</sub> values of 26.43 ± 1.84 µg/mL (leaf) and 34.41 ± 1.42 µg/mL (stem). Molecular docking (AutoDock Vina 1.1.2) was performed to explore interactions between key compounds and inducible nitric oxide synthase (iNOS), cyclooxygenase-2 (COX-2), and interleukin-8 (IL-8). Dodecanal, β-vetivenene, neryl isovalerate, and khusilal showed favourable binding affinities, with β-vetivenene exhibiting the strongest interaction with iNOS. This is the first report on the essential oils of *I. celebica*, highlighting their promising natural anti-inflammatory potential.

## 1 | Introduction

*Illigera* Blume is a genus belonging to the family Hernandiaceae [1]. According to *Flora of the World Online*, this genus includes 28 species widely distributed across tropical and subtropical regions [2]. The species of this genus are found from tropical Africa and Madagascar to tropical and subtropical Asia. They are commonly observed in tropical moist forests, particularly at low to medium altitudes [2].

The *Illigera* genus offers promising pharmaceutical potential. In traditional Chinese medicine, several species of the genus *Illigera*,

such as *Illigera grandiflora*, *Illigera cordata*, *Illigera aromatica*, *Illigera luzonensis*, and *Illigera rhodantha*, have also been used to treat various inflammatory diseases such as rheumatic arthralgia and conjunctivitis [3–6]. Numerous studies have reported that plants within this genus contain biologically active natural compounds, such as flavonoids, alkaloids, and essential oils [7]. These compounds exhibit notable pharmacological activities, including anti-inflammatory, antibacterial, and antioxidant effects, which enhance the scientific and medicinal value of the genus *Illigera* in medicine and phytochemistry [8–10]. Despite this potential, studies on specific species within the genus, particularly *Illigera celebica*, remain limited.



**FIGURE 1** | *Illigera celebica* Hance. (Hernandiaceae).

*I. celebica* (Figure 1) is an evergreen woody liana characterized by angular glabrous stems; ternate leaves with papery or leathery ovate-elliptic leaflets; cymose inflorescences measuring 15–20-cm long; and distinctive four-winged fruits [11]. This species is found primarily in the southern provinces of China (Yunnan, Guangxi, and Guangdong) and Southeast Asia, including Vietnam, Thailand, and Cambodia [12].

In Vietnamese traditional medicine, *I. celebica* is used to treat rheumatism and paralysis [13]. Although its presence is well-documented, scientific investigations into its chemical composition and biological activities are notably limited. This lack of data contrasts sharply with the known bioactivity of other species in the genus, suggesting untapped potential in *I. celebica* for pharmaceutical and phytochemical applications.

This study aims to elucidate the essential oil composition from the leaves and stems of *I. celebica* and assess its inhibitory activity on nitric oxide (NO) production. The findings are expected to provide valuable insights into this plant's medicinal and chemical potential. To the best of our knowledge, this study represents the first detailed investigation of the essential oil composition and biological activities of *I. celebica*. While several species of the *Illigera* genus have been studied for their bioactive constituents, no prior reports have focused on the essential oils of *I. celebica*. Our findings not only fill this gap in the literature by elucidating the chemical profiles of leaf and stem essential oils but also provide insight into their promising anti-inflammatory activity and molecular interactions with key targets. This work paves the way for future in-depth studies on the pharmacological applications of *I. celebica* essential oil, including in vivo validation and exploration of potential synergistic effects with conventional therapies. Furthermore, the observed differences in chemical composition between plant parts highlight the need for further studies on geographical and seasonal variations in essential oil yield and composition.

## 2 | Results and Discussion

### 2.1 | Chemical Composition of *I. celebica* Essential Oil

The essential oil yield was  $1.20 \pm 0.01\%$  (w/w) of fresh weight in the leaves and  $0.08 \pm 0.02\%$  (w/w) of fresh weight in

the stems. In total, 20 compounds, primarily belonging to the aldehyde and oxygenated sesquiterpene groups, were identified in the essential oils of these two parts. The leaf essential oil (Table 1) contained eight compounds classified into alkane (11.5%), aldehyde (65.9%), sesquiterpene hydrocarbon (5.2%), and oxygenated sesquiterpene (5.6%) groups, with dodecanal (65.9%) as the predominant component. The stem essential oil (Table 1) contained 15 compounds distributed among alkane (2.6%), aldehyde (40.9%), sesquiterpene hydrocarbon (0.5%), oxygenated sesquiterpene (40.3%), and diterpene (0.9%) groups, with dodecanal (33.4%) and khusimone (31.5%) as the main components.

The variation in the proportions of some compounds between the leaves and stems is a notable highlight. For instance, dodecanal accounted for 65.9% in the leaves but decreased to 33.4% in the stems, whereas khusimone sharply increased from 6.2% in the leaves to 31.5% in the stems. Certain compounds, such as tetradecanal, also exhibited differing proportions (2.6% in the leaves compared to 7.5% in the stems). Aldehydes were the dominant group in the leaves, with dodecanal as the primary component. In addition, alkanes formed a significant portion of the leaf essential oil, with *n*-tridecane accounting for 11.5%. The presence of compounds such as (*E*)- $\beta$ -farnesene and  $\beta$ -vetivenene further contributed to the unique chemical profile of the leaf essential oil.

In contrast, the stem essential oil, although containing a lower proportion of aldehydes than the leaf essential oil, was notable for its high oxygenated sesquiterpene content (40.3%), with khusimone being the most abundant compound. The composition of the stem essential oil was also more diverse, featuring characteristic compounds such as *trans*-2-*tert*-butyl-cyclohexanol acetate, 11-acetoxyeudesman-4- $\alpha$ -ol, and tetradecanal. Notably, the proportion of sesquiterpene hydrocarbons in the leaves (5.2%) was significantly higher than in the stems (0.5%), whereas the oxygenated sesquiterpene content in the stems (40.3%) far exceeded that in the leaves (5.6%).

The differences in essential oil composition between the leaves and stems may reflect the biological adaptation of the plant, with each part performing distinct functions. These significant variations are evident in the proportions of major compound groups and the presence of specific characteristic compounds. This highlights the potential for utilizing essential oils from different parts of the plant for diverse applications in the pharmaceutical, cosmetic, and food industries.

To date, research on the essential oils of the *Illigera* genus remains limited. The essential oil extracted from the leaves and stems of *I. trifoliata* ssp. *cucullata* is characterized by a high concentration of monoterpene hydrocarbons, particularly  $\alpha$ -pinene and  $\alpha$ -phellandrene [14]. Similarly, the essential oil from *I. aromatica* has been reported to be rich in  $\alpha$ -pinene,  $\beta$ -pinene,  $\alpha$ -phellandrene, *p*-cymene,  $\beta$ -phellandrene,  $\alpha$ -bisabolene and  $\alpha$ -eudesmol [15]. These findings highlight the remarkable diversity in the essential oil profiles of the *Illigera* genus.

**TABLE 1** | Chemical composition of the essential oil from leaves and stems of *Illigera celebica*.

No	RT	Compounds <sup>a</sup>	RI <sup>b</sup>	RI <sup>c</sup>	Concentration %	
					Leaf	Stem
1	21.84	<i>n</i> -Tridecane	1302	1300	<b>11.5</b>	—
2	22.83	<i>trans</i> -2- <i>tert</i> -butyl-Cyclohexanol acetate	1325	1312	—	3.2
3	25.69	1-Tetradecene	1391	1388	—	1.9
4	27.21	Dodecanal	1428	1408	65.9	33.4
5	27.71	Aromadendrene	1440	1439	—	0.5
6	29.21	( <i>E</i> )- $\beta$ -Farnesene	1477	1454	1.5	—
7	31.36	Isobornyl isovalerate	1530	1521	—	0.9
8	32.31	$\beta$ -Vetivenene	1555	1554	3.7	—
9	32.49	Longicamphenylone	1559	1562	2.8	—
10	33.11	Caryophyllene oxide	1575	1582	—	1.0
11	33.48	Neryl isovalerate	1585	1582	2.8	—
12	34.32	Khusimone	1605	1604	6.2	31.5
13	35.33	Tetradecanal	1626	1611	2.6	7.5
14	36.19	allo-Aromadendrene epoxide	1644	1639	—	0.3
15	36.34	Khusilal	1648	1647	—	1.4
16	37.13	14-hydroxy-( <i>Z</i> )-Caryophyllene	1664	1666	—	2.8
17	37.63	Khusilol	1675	1675	—	2.4
18	41.56	<i>n</i> -Octadecane	1806	1800	—	0.6
19	46.08	11-Acetoxyeudesman-4- $\alpha$ -ol	1941	1938	—	3.0
20	47.23	1-Eicosene	1977	1987	—	0.9
Alkane (A)					1.2	2.6
Aldehyde (AD)					65.9	40.9
Sesquiterpene hydrocarbon (S)					5.2	0.5
Oxygenated sesquiterpene (OS)					5.6	40.3
Diterpene					—	0.9
Others (O)					8.8	6.1
Total					97.0	91.3

<sup>a</sup>Elution order on Equity-5 column.<sup>b</sup>Retention Indices on Equity-5 column.<sup>c</sup>Literature retention indices, standard compounds.

## 2.2 | Inhibitory no Production of *I. celebica* Leaves and Stems Essential Oil

The findings (Table 2) indicate that the essential oils derived from the leaves and stems of *I. celebica* exhibit appreciable inhibitory activity against NO production, with IC<sub>50</sub> values of  $26.43 \pm 1.84$  and  $34.41 \pm 1.42$   $\mu\text{g/mL}$ , respectively, whereas the positive control, dexamethasone, exhibited a stronger effect, with an IC<sub>50</sub> value of  $13.96 \pm 1.38$   $\mu\text{g/mL}$ . Although both samples were active, the leaf oil (ICL) demonstrated greater potency than the stem oil (ICS) ( $p = 0.0049$ ), while both were less effective than the positive control ( $p = 0.0010$  and  $p = 0.0001$  for ICL and ICS, respectively).

To ensure that the observed NO inhibition was not due to general cytotoxicity, we conducted parallel cytotoxicity assays using the 3-(4, 5-dimethylthiazol-2-yl)-2,5-diphenyltetrazolium

bromide (MTT) assay. After measuring NO levels, the remaining cells in each well were incubated with MTT solution, and cell viability was determined. At the highest tested concentration (100  $\mu\text{g/mL}$ ), the cell viability remained high, at  $92.42 \pm 3.4\%$  for the leaf essential oil and  $100.87 \pm 1.24\%$  for the stem essential oil. This demonstrates that the NO inhibition by *I. celebica* essential oils occurred at concentrations that did not compromise cell viability, confirming that the observed inhibitory activity is independent of general cytotoxic effects.

Compared to standard anti-inflammatory drugs and other known essential oils, the *I. celebica* essential oils showed promising activity. Specifically, dexamethasone as the positive control exhibited an IC<sub>50</sub> of  $13.96 \pm 1.38$   $\mu\text{g/mL}$ , which was lower than the IC<sub>50</sub> values of the *I. celebica* essential oils ( $26.43 \pm 1.84$   $\mu\text{g/mL}$  for leaves and  $34.41 \pm 1.42$   $\mu\text{g/mL}$  for stems). While less potent

**TABLE 2** | NO inhibitory activity of *Illigera celebica* leaves and stems essential oil.

C (μg/mL)	ICL		ICS		Dexamethasone	
	% I	% CS	% I	% CS	% I	% CS
100	93.83 ± 2.48	92.42 ± 3.40	89.90 ± 1.35	100.87 ± 1.24	89.26 ± 1.55	92.09 ± 1.54
20	41.73 ± 2.01	104.45 ± 2.56	34.48 ± 1.09	102.93 ± 0.97	53.64 ± 1.07	101.03 ± 1.68
4	19.26 ± 1.25		17.24 ± 0.82		41.27 ± 0.82	
0.8	1.18 ± 0.11		8.37 ± 0.39		32.92 ± 0.89	
IC <sub>50</sub>	26.43 ± 1.84		34.41 ± 1.42		13.96 ± 1.38	

Note: Data are shown as mean ± standard deviation ( $n = 3$ ).

% CS, % cell survival; % I, % inhibition; C, concentration; dexamethasone, positive control; IC<sub>50</sub>, half-maximal inhibitory concentration; ICL, *I. celebica* leaves essential oil; ICS, *I. celebica* stems essential oil.

than dexamethasone, the essential oils of *I. celebica* demonstrated comparable activity to other essential oils previously reported for NO inhibition. For instance, the essential oil from *I. rhodantha* had an IC<sub>50</sub> of 21.13 ± 1.27 μg/mL [16], and *Litsea balansae* essential oil showed an IC<sub>50</sub> of 28.09 ± 1.53 μg/mL [17], both of which are similar to *I. celebica* essential oils in this study.

These results highlight the strong NO-inhibitory potential and the high safety profile of *I. celebica* essential oils, underscoring their promise for further pharmacological research and development applications.

### 2.3 | Molecular Docking Study

NO functions as a crucial inflammatory mediator and serves as a physiological signaling molecule and an intracellular chemical messenger in the body. NO significantly influences the regulation of inflammatory responses, especially when produced at high levels by macrophages after stimulation by lipopolysaccharide (LPS) [18]. Therefore, compounds capable of inhibiting LPS-induced NO production are considered potential candidates for anti-inflammatory therapy. The evaluation of the NO inhibitory activity of essential oil extracted from the leaves and stems of *I. celebica* has demonstrated promising applications in inflammation treatment. To elucidate the mechanism of action, the essential oil components were studied using molecular docking, focusing on three key inflammatory targets: inducible nitric oxide synthase (iNOS), cyclooxygenase-2 (COX-2), and interleukin-8 (IL-8). The aim of this analysis was to identify the molecular mechanisms contributing to the anti-inflammatory effects of the essential oil. The use of molecular docking models has been widely applied in recent studies to investigate the interactions between essential oil constituents and various enzyme targets, demonstrating the applicability of in silico approaches in natural product research [19, 20].

Docking results (Table 3) indicated that all essential oil components exhibited negative binding affinities with the target enzymes, reflecting their potential beneficial biological interactions. Dodecanal, the most abundant compound in *I. celebica* essential oil from leaves (65.9%) and stems (33.4%), showed favorable interactions with iNOS (−6 kcal/mol) and COX-2 (−5.8 kcal/mol). Although it was not the compound with the lowest docking score, its high proportion in the essential oil

suggests that dodecanal may play a major role in its in vitro anti-inflammatory activity, particularly through NO inhibition. Docking analysis revealed that dodecanal formed hydrogen bonds with Arg199 and engaged in hydrophobic interactions with key amino acids such as Cys200, Trp194, Phe369, Leu209, Ala197, Tyr489, and Met355 (Figure 2).

Beyond dodecanal, several other minor constituents also exhibited strong affinities for iNOS. Notably, β-vetivenene (−9.7 kcal/mol) had the lowest docking score against iNOS, suggesting potent inhibitory potential, especially when compared to the reference compound dexamethasone (−8.7 kcal/mol). Despite not forming hydrogen bonds, β-vetivenene participated in multiple hydrophobic interactions with important amino acids, including Cys200, Pro350, Leu209, Phe369, and Trp194 (Figure 3). In addition, some other compounds, such as neryl isovalerate (−8.5 kcal/mol) and khusilal (−8.5 kcal/mol), exhibited strong binding affinities, contributing significantly to iNOS inhibition. Khusilol (−8 kcal/mol) and (E)-β-farnesene (−8.1 kcal/mol) also showed potential for enhancing the anti-inflammatory effect.

For the COX-2 target, an enzyme crucial in prostaglandin synthesis, which mediates swelling, pain, and fever, khusilal (−8 kcal/mol) and (E)-β-farnesene (−7 kcal/mol) exhibited equivalent docking scores to dexamethasone (−7.2 kcal/mol), indicating strong COX-2 inhibition potential. Dexamethasone was included as a reference compound in the docking simulations to benchmark binding affinities, as it is a well-established anti-inflammatory agent also used in the in vitro NO inhibition assay. The comparable or stronger binding scores of certain essential oil constituents, particularly with COX-2, support their potential relevance to the observed biological activity and reinforce the predictive value of the docking results.

Regarding the IL-8 target, a chemokine that plays a key role in neutrophil recruitment to inflammation sites, khusilal (−7.2 kcal/mol) and khusilol (−6.8 kcal/mol) have favorable binding affinities toward IL-8, suggesting their potential to inhibit its activity. This inhibition may help reduce neutrophil recruitment, thus limiting excessive inflammatory responses.

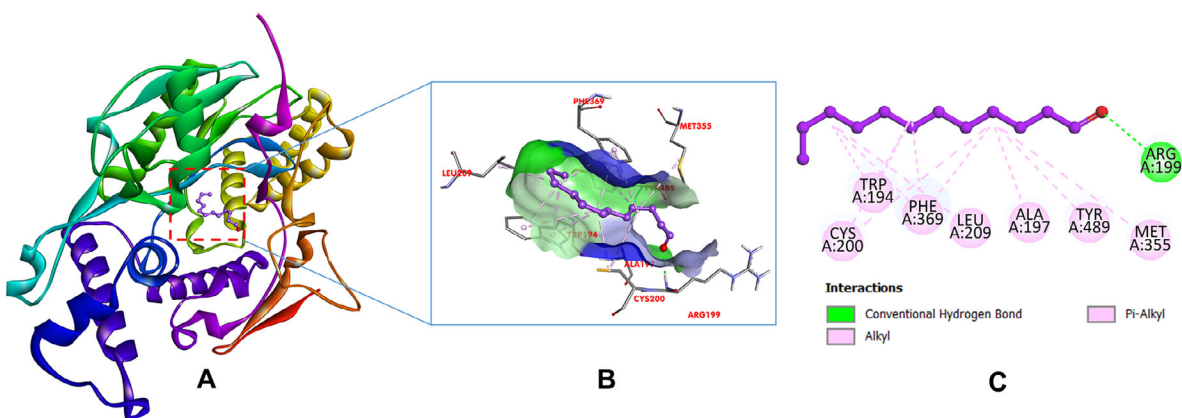
Despite the promising in silico results, this study has certain limitations. While molecular docking provided valuable insights into the potential interactions between essential oil constituents and inflammation-related protein targets, further validation using

TABLE 3 | Docking score between the compounds and the proteins.

No	Compounds	Docking score (kcal/mol)		
		iNOS	COX-2	IL-8
1	<i>n</i> -Tridecane	-6.4	-5.6	-4.4
2	<i>trans</i> -2- <i>tert</i> -butyl-Cyclohexanol acetate	-5.9	-5.8	-5.8
3	1-Tetradecene	-6.6	-6	-5
4	Dodecanal	-6	-5.8	-4.5
5	Aromadendrene	-7.4	-7.5	-6.6
6	( <i>E</i> )- $\beta$ -Farnesene	-8.1	-7	-5.9
7	Isobornyl isovalerate	-7.1	-7.1	-5.8
8	$\beta$ -Vetivenene	-9.7	-7.4	-7.3
9	Longicamphenylone	-6.3	-6.5	-6.7
10	Caryophyllene oxide	-6.6	-6.2	-5.9
11	Neryl isovalerate	-8.5	-7.3	-5.8
12	Khusimone	-6.4	-6.9	-6.2
13	Tetradecanal	-6.6	-5.8	-4.6
14	allo-Aromadendrene epoxide	-7	-6.7	-6.7
15	Khusilal	-8.5	-8	-7.2
16	14-hydroxy-( <i>Z</i> )-Caryophyllene	-6.9	-6.3	-6.4
17	Khusilol	-8	-7.2	-6.8
18	<i>n</i> -Octadecane	-5.9	-6.5	-4.6
19	11-Acetoxyeudesman-4- $\alpha$ -ol	-7	-6.7	-6.8
20	1-Eicosene	-6.9	-6.7	-4.6
21	Dexamethasone <sup>a</sup>	-8.7	-7.2	-7.1

<sup>a</sup>Dexamethasone used as a reference anti-inflammatory drug.





**FIGURE 2** | Interaction analysis between iNOS (PDB: 3E7G) and dodecanal using Discovery Studio 2024.1. (A) 3D overall structure of the iNOS–dodecanal complex showing the ligand binding site. (B) 3D close-up view of the binding pocket with dodecanal and interacting residues. (C) 2D interaction diagram of dodecanal within the iNOS active site.

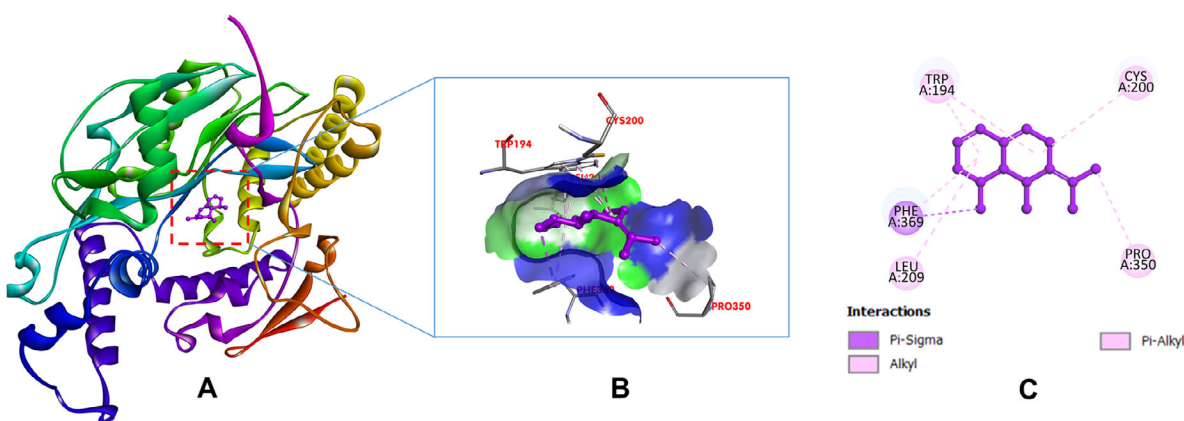


**FIGURE 3** | Interaction analysis between iNOS (PDB: 3E7G) and  $\beta$ -vetivenene using Discovery Studio 2024.1. (A) 3D overall structure of the iNOS– $\beta$ -vetivenene complex showing the ligand binding site. (B) 3D close-up view of the binding pocket with  $\beta$ -vetivenene and interacting residues. (C) 2D interaction diagram of  $\beta$ -vetivenene within the iNOS active site.

molecular dynamics simulations could help evaluate the conformational stability and binding persistence of the ligand–protein complexes over time. In addition, expression-level analyses of key inflammatory markers such as iNOS, COX-2, and IL-8 in treated cells would provide direct experimental confirmation of the proposed mechanisms. These complementary approaches were beyond the scope of the current study but will be considered in future investigations to strengthen the mechanistic understanding of *I. celebica*'s anti-inflammatory potential.

This study addresses a significant gap in the current literature by reporting the essential oil composition and anti-inflammatory properties of *I. celebica* for the first time. These findings contribute to a better understanding of the chemical diversity and potential therapeutic applications of this species.

### 3 | Conclusions

This study presents the first report on the chemical composition and in vitro NO production inhibitory activity of *I. celebica* essential oils, filling a critical gap in the existing literature. Our findings indicate that the essential oil of *I. celebica* shows promising anti-inflammatory activity, supported by significant

NO inhibition and molecular docking results. Key bioactive components—such as dodecanal,  $\beta$ -vetivenene, neryl isovalerate, and khushil—demonstrated strong interactions with important inflammatory targets (iNOS, COX-2, and IL-8), suggesting a multi-target mechanism of action. These results contribute valuable insights into the chemical diversity and pharmacological potential of the *Illigera* genus.

Nevertheless, a limitation of our current study is the absence of direct experimental validation of protein expression (e.g., iNOS, COX-2) or in vivo testing. Future work should incorporate animal models of inflammation and protein-level analyses (such as Western blot or qPCR) to confirm the predicted molecular interactions and fully establish the therapeutic relevance of *I. celebica* essential oils.

### 4 | Experimental Section

#### 4.1 | Plant Materials

The fresh leaves (1.0 kg) and fresh stems (1.0 kg) of *I. celebica* were collected from Dakrong district, Quang Tri province in September

2024 (16°39'40.0" N, 106°49'23.1" E), and identified by Dr. Le Tuan Anh, Viet Nam National Museum of Nature. A voucher specimen (IC\_02) has been deposited in the Faculty of Pharmacy at Hue University of Medicine and Pharmacy, Hue University, Vietnam.

## 4.2 | Materials

LPSs from *Escherichia coli*, sodium nitrite, sulfanilamide, *N*-1-naphthylethylenediamine dihydrochloride and dimethyl sulfoxide (DMSO) from Sigma Chemical Co. (St. Louis, MO, USA) were obtained from Sigma Chemical Co. Dulbecco's modified Eagle's medium (DMEM), fetal bovine serum (FBS) were from Life Technologies, Inc. (Gaithersburg, MD, USA).

## 4.3 | Cell Source and Culture

RAW 264.7 cell lines were kindly provided by Prof. Dr. Domenico Delfino, University of Perugia, Perugia, Italy. Stock cultures were cultured in DMEM medium supplemented with 2 mM L-glutamine, 10 mM HEPES, 1.0 mM sodium pyruvate, and 10% FBS (GIBCO). The cells were subcultured every 3–5 days at a 1:3 ratio and maintained in a CO<sub>2</sub> incubator under controlled conditions of 37°C and 5% CO<sub>2</sub>.

## 4.4 | Hydrodistillation of the Essential Oils

Following methods established in previous works [21–23], before the hydrodistillation process, the fresh leaves of *I. celebica* were shredded. Samples were then subjected to hydrodistillation using a Clevenger apparatus for three hours at normal pressure, according to [24]. The essential oils were then collected and dried by sodium sulfate (Na<sub>2</sub>SO<sub>4</sub>) and then stored in a refrigerator at 4°C. The experiments were repeated in triplicate.

## 4.5 | Analysis of the Essential Oil

The composition of the essential oil was determined using the GCMS-QP2010 Plus system from Shimadzu (Kyoto, Japan). This system featured an Equity-5 capillary column with dimensions of 30 meters in length and 0.25 mm in diameter, coated with a 0.25-μm-thick film. Gas chromatography–mass spectrometry (GC/MS) analysis was conducted using a mass spectrometer (MSD QP2010 Plus). Before analysis, the essential oil was diluted in *n*-hexane at a 1:100 ratio, and 1 μL of this diluted solution was injected. Helium served as the carrier gas at a constant flow rate of 1.5 mL/min. The injector and interface temperatures were both maintained at 280°C. The column temperature program started at 60°C (held for 2 min), then increased to 240°C at a rate of 3°C/min (held for 10 min), followed by a rise to 280°C at 5°C/min (held for 40 min). The injection was performed in splitless mode. The mass spectrometer operated at an ionization voltage of 70 eV, scanning mass-to-charge ratios (*m/z*) in the range of 45–500 with a sampling rate of 1.0 scan/s.

Compound identification was achieved by comparing the mass spectral data with known fragmentation patterns available in the literature [25]. In addition, retention indices (RI Exp.) were

determined using a homologous series of *n*-alkanes (C8–C38) under identical GC conditions. Some compounds were further identified through co-injection with standard compounds under the same analytical conditions. The relative peak area percentage was used for quantification.

## 4.6 | NO Inhibition Assay

Cells were seeded at a density of 2 × 10<sup>5</sup> cells/well in 96-well plates and incubated at 37°C with 5% CO<sub>2</sub> for 24 h. Following incubation, the culture medium was replaced with FBS-free DMEM. Samples at varying concentrations were then added to the wells in the presence of LPS (1 μg/mL) and incubated for an additional 24 h. Dexamethasone (Sigma) was utilized as the positive control, while 1.0% diluted DMSO served as the negative control. Nitrite levels, as a proxy for NO production, were quantified using the Griess reagent system (Promega Corporation, WI, USA). Specifically, 100 μL of the culture supernatant was transferred to a new 96-well plate, followed by the addition of 100 μL of Griess reagent, comprising 50 μL of 1% (w/v) sulfanilamide in 5% (v/v) phosphoric acid and 50 μL of 0.1% (w/v) *N*-1-naphthylethylenediamine dihydrochloride. The reaction mixture was incubated at room temperature for 10 min, and nitrite concentration was determined by measuring the absorbance at 540 nm using a microplate reader. The inhibitory activity of the samples on NO production was evaluated at essential oil concentrations of 100, 20, 4, and 0.8 μg/mL. The IC<sub>50</sub> values were calculated using Table Curve Version 4.0 (Systat Software Inc., San Jose, CA, USA) [26].

## 4.7 | MTT Cell Viability Assay

The cell culture plate used for the NO expression assay, after collecting the supernatant to determine NO levels, was supplemented with 90 μL of cell culture medium and 10 μL of MTT (final concentration: 5 mg/mL) per well. After 4 h, the medium was removed, and the formazan crystals were dissolved using 50 μL of 100% DMSO.

The OD values were measured at a wavelength of 540 nm using a BioTek Elx800 microplate reader. The cell viability in the presence of the tested substances was determined using the following formula:

$$\text{Inhibition (\%)} = \frac{\text{OD (sample)} - \text{OD (blank)}}{\text{OD (DMSO)} - \text{OD (blank)}}$$

## 4.8 | Molecular Docking Study

Molecular docking simulations were conducted using AutoDock Vina 1.1.2 [27] running on a Windows 11 system powered by a 3.40 GHz Intel Core i5 processor. This program employs a semi-empirical scoring function, combining empirical and knowledge-based terms calibrated to approximate ligand–protein binding affinities.

The three key target proteins included iNOS (PDB ID: 3E7G) [28], COX-2 (PDB ID: 5KIR) [29], and IL-8 (PDB ID: 5D14)

[30] were sourced from the Protein Data Bank and preprocessed in AutoDock Tools 1.5.7. This preparation involved the removal of water molecules and non-essential ligands, followed by the assignment of Kollman charges to ensure proper docking simulations.

Ligand structures were meticulously designed using ChemDraw 16.0, converted into 3D conformations, and energy-minimized through Open Babel 3.1.1 [31] to enhance their stability. Dexamethasone, a well-known anti-inflammatory drug, was included as a reference inhibitor to provide a benchmark for evaluating the docking performance of the essential oil constituents. The accuracy of the docking procedure was validated by comparing the root mean square deviation (RMSD) between the crystallographic and docked poses, with all values remaining below 2 Å, confirming the protocol's reliability.

Post-docking analysis was performed to examine hydrogen bonding, hydrophobic contacts, and other key interactions at the active sites. All docking poses were carefully inspected to ensure the plausibility of the binding conformations, using visualization and interaction tools integrated in Discovery Studio 24.1.

## 4.9 | Statistical Analysis

Means with standard deviation were reported for each measurement in three replicates. Student's *t*-test with a significance level of  $p < 0.05$  was used to statistically compare the data.

### Author Contributions

**Linh Thuy Thi Tran:** Conceptualization, Supervision, Investigation, Molecular modeling, Formal analysis, Original draft preparation, Writing – review and editing, Data curation. **Trang Huyen Xuan Hoang:** Conceptualization, Investigation, Data curation, Original draft preparation, Writing – review and editing, Formal analysis. **Tuan Quoc Doan:** Methodology, Sampling and extraction, Investigation, Data curation, Original draft preparation. **The-Huan Tran:** Methodology, Investigation, Molecular modeling, Original draft preparation. **Hoai Thi Nguyen:** Methodology, Investigation, Original draft preparation. **Anh Tuan Le:** Sampling and extraction, Plant identification.

### Acknowledgments

Tran The Huan was funded by the Master PhD Scholarship Programme of Vingroup Innovation Foundation (VINIF), code VINIF.2024.TS.053.

### Conflicts of Interest

The authors declare no conflicts of interest.

### Data Availability Statement

The data that support the findings of this study are available in the [Supporting Information](#) of this article.

### References

1. R. Govaerts, E. Nic Lughadha, N. Black, R. Turner, and A. Paton, "The World Checklist of Vascular Plants, a Continuously Updated Resource for Exploring Global Plant Diversity," *Scientific Data* 8 (2021): 215.

2. "Illigera Blume | Plants of the World Online | Kew Science," accessed December 31, 2024, <http://powo.science.kew.org/taxon/urn:lsid:ipni.org:names>.

3. K. S. Chen, Y. C. Wu, C. M. Teng, F. N. Ko, and T. S. Wu, "Bioactive Alkaloids From *Illigera luzonensis*," *Journal of Natural Products* 60 (1997): 645–647.

4. J.-J. Chen, H.-C. Hung, P.-J. Sung, I.-S. Chen, and W.-L. Kuo, "Aporphine Alkaloids and Cytotoxic Lignans From the Roots of *Illigera luzonensis*," *Phytochemistry* 72 (2011): 523–532.

5. J.-W. Dong, L. Cai, X.-J. Li, et al., "Fermentation of *Illigera aromatica* With *Clonostachys rogersoniana* Producing Novel Cytotoxic Menthane-Type Monoterpenoid Dimers," *RSC Advances* 7 (2017): 38956–38964.

6. J.-W. Dong, L. Cai, X.-J. Li, J.-P. Wang, R.-F. Mei, and Z.-T. Ding, "Monoterpene Esters and Aporphine Alkaloids From *Illigera aromatica* With Inhibitory Effects Against Cholinesterase and NO Production in LPS-Stimulated RAW264.7 Macrophages," *Archives of Pharmacol Research* 40 (2017): 1394–1402.

7. L. M. Conserva, C. d. A. B. Pereira, and J. M. Barbosa-Filho, "Alkaloids of the Hernandiaceae: Occurrence and a Compilation of Their Biological Activities," in *The Alkaloids: Chemistry and Biology*, ed. G. A. Cordell (Academic Press, 2005), 175–243.

8. X.-J. Li, J.-W. Dong, L. Cai, R.-F. Mei, and Z.-T. Ding, "Improving the Acetylcholinesterase Inhibitory Effect of *Illigera henryi* by Solid-State Fermentation With *Clonostachys rogersoniana*," *Journal of Bioscience and Bioengineering* 124 (2017): 493–497.

9. X.-Y. Pu, K. Tian, J.-X. Sun, et al., "Anti-inflammatory Monoterpene Esters From the Stems of *Illigera aromatica*," *Natural Product Research* 35 (2021): 960–966.

10. C.-H. Huang, Y.-Y. Chan, P.-C. Kuo, et al., "The Constituents of Roots and Stems of *Illigera luzonensis* and Their Anti-Platelet Aggregation Effects," *International Journal of Molecular Sciences* 15 (2014): 13424–13436.

11. X. Li, J. Li, and E. E. D. Brigitta, "Flora of China," *Illigera Celebica Flora China* 259 (1866).

12. Y. Xin, J. Xin, G. Yao, et al., "The Complete Chloroplast Genome Sequence of *Illigera celebica*," *Mitochondrial DNA Part B* 5 (2020): 2454–2455.

13. National Institute of Medical Materials, *Checklist of Medicinal Plants in Vietnam* (Science And Technics Publishing House, 2016).

14. T. Huy, N. Hiên, N. Hung, J. Casanova, M. Paoli, and F. Tomi, "Integrated Analysis of Vietnamese *Illigera trifoliata* ssp. *Cucullata* (Merr.) Kubitzki, Leaf and Stem Essential Oils by GC-FID/GC-MS and <sup>13</sup>C NMR," *Records of Natural Products* 16 (2022): 657–662.

15. S. Mo, Z. Li, Y. Ou, S. Wei, X. Si, and D. Fan, "Chemical Components of Essential Oil in the *Illigera aromatica* S.Z.Huang Et S.L.Mo by GC-MS," *Lishizhen Medicine and Materia Medica Research* 17 (2006): 2512–2513.

16. T. Q. Doan, H. T. Nguyen, T. H. X. Hoang, T. Y. Nhu Thi Nguyen, A. T. Le, and L. T. T. Tran, "Chemical Composition and Biological Activities of Essential Oil From *Illigera rhodantha* Hance. (Hernandiaceae) From Vietnam," *Journal of Essential Oil-Bearing Plants* 28 (2025): 331–339.

17. D. V. Ho, H. N. T. Hoang, N. H. Nguyen, et al., "GC-MS Characterization, In Vitro Antioxidant and Anti-Inflammatory Activities of Essential Oil From the Leaves of *Litsea balansae* Lecomte," *Natural Products Communications* 18 (2023): 1934578X231214159.

18. J. L. Schultze, A. Schmieder, and S. Goerdts, "Macrophage Activation in human Disease," *Seminars in Immunology* 27 (2015): 249–256.

19. G. Nouioura, M. El fadili, N. El Hachlafi, et al., "Coriandrum sativum L., Essential Oil as a Promising Source of Bioactive Compounds With GC/MS, Antioxidant, Antimicrobial Activities: In Vitro and In Silico Predictions," *Frontiers in Chemistry* 12 (2024): 1369745.



20. G. Nouioura, M. El fadili, N. El Hachlafi, et al., "Petroselinum crispum L., Essential Oil as Promising Source of Bioactive Compounds, Antioxidant, Antimicrobial Activities: *In Vitro* and *In Silico* Predictions," *Heliyon* 10 (2024): e29520.
21. D. Q. Tuan, D. Dien, T. V. Pham, et al., "Chemical Composition of Essential Oil From the Rhizomes and Leaves of *Newmania sontraensis* H.Đ.Trân, Luu & Škornick (Zingiberaceae) From Vietnam," *Journal of Essential Oil-Bearing Plants* 24 (2021): 1260–1268.
22. D. Q. Tuan, D. Dinh, T. N. Tran, et al., "Chemical Composition of Essential Oil From the *Zingiber monophyllum* (Zingiberaceae) From Vietnam," *Journal of Essential Oil-Bearing Plants* 25 (2022): 987–993.
23. T. Q. Doan, D. V. Ho, N. Trong Le, et al., "Chemical Composition and Anti-Inflammatory Activity of the Essential Oil From the Leaves of *Limnocitrus littoralis* (Miq.) Swingle From Vietnam," *Natural Product Research* 35 (2021): 1550–1554.
24. *Vietnamese Pharmacopoeia V* (Medical Publishing House, 2017).
25. R. P. Adams, *Identification of Essential Oil Components by Gas Chromatography/Mass Spectrometry* (Allured Publishing, 2017).
26. H. Liao, L. Banbury, H. Liang, et al., "Effect of Honghua (*Flos carthami*) on Nitric Oxide Production in RAW 264.7 Cells and  $\alpha$ -Glucosidase Activity," *Journal of Traditional Chinese Medicine* 34 (2014): 362–368.
27. O. Trott and A. J. Olson, "AutoDock Vina: Improving the Speed and Accuracy of Docking With a New Scoring Function, Efficient Optimization and Multithreading," *Journal of Computational Chemistry* 31 (2010): 455–461.
28. E. D. Garcin, A. S. Arvai, R. J. Rosenfeld, et al., "Anchored Plasticity Opens Doors for Selective Inhibitor Design in Nitric Oxide Synthase," *Nature Chemical Biology* 4 (2008): 700–707.
29. B. J. Orlando and M. G. Malkowski, "Crystal Structure of rofecoxib Bound to human Cyclooxygenase-2," *Acta Crystallographica Section F, Structural Biology Communications* 72 (2016): 772.
30. K. Brzezinski, Y. Pompeu, S. Lu, J. Jakoncic, and D. A. Ostrov, "The Atomic Resolution Crystal Structure of Human IL-8," Protein Data Bank Structure ID-5D 14, <https://doi.org/10.2210/pdb5D14/pdb>.
31. N. M. O'Boyle, M. Banck, C. A. James, C. Morley, T. Vandermeersch, and G. R. Hutchison, "Open Babel: An Open Chemical Toolbox," *Journal of Cheminformatics* 3 (2011): 33.

## Supporting Information

Additional supporting information can be found online in the Supporting Information section.

cbdv70242-sup-0001-FigureS1-S5.pdf